JOURNAL OF Materials CHEMISTRY

A new route to γ-Fe_2O_3 *via* an intermediate oxyhydroxide. The reaction of α-$NaFeO_2$ with benzoic acid†

M. C. Blesa,[a] E. Morán,*[a] J. D. Tornero,[b] N. Menéndez,[b] E. Mata-Zamora[c] and J. M. Saníger[c]

[a]*Dpto. Química Inorgánica, Fac. Ciencias Químicas, Universidad Complutense, 28040 Madrid, Spain*
[b]*Dpto. Química-Física Aplicada, Fac. Ciencias, Universidad Autónoma Cantoblanco, 28049 Madrid, Spain*
[c]*Centro de Instrumentos, Universidad Autónoma de México, 04510 México, D.F., México*

Received 28th April 1998, Accepted 16th July 1998

Proton exchange reactions have been performed on α-$NaFeO_2$ at 150 °C in molten benzoic acid; a ferrimagnetic material showing the spinel structure was produced. Infrared spectroscopy was used to investigate the oxyhydroxide character of this product which, after thermal treatment at 300 °C yields the well known maghemite γ-Fe_2O_3, although some hydroxyl groups still seem to be present. Besides IR, X-ray diffraction, chemical and thermal analysis, Mössbauer spectroscopy and magnetization measurements are presented and discussed.

Introduction

Cation exchange reactions performed on many materials, especially those which are fast ion conductors, offer a preparative route to new, very often metastable, compounds. Taking into account the moderate temperatures at which these exchanges are usually performed, they can be considered as a '*chimie douce*' method of preparation. For obvious reasons, most of the studies devoted to this topic deal with metal oxides. Thermodynamic and kinetic aspects are of great relevance in this context and, from the structural point of view, the ease of the exchange is related to the 'open' character of the solid matrix: interconnected cages, channels or layers of sufficient dimensions favor cationic diffusion. For reasons of charge and, therefore, mobility, monovalent cations (alkali metal, Cu^+, Ag^+, In^+, Tl^+, *etc.*) are much more easily exchanged and this has been well documented in the literature.[1,2]

In this connection and in a formal sense, the replacement of alkali metal cations by protons could be considered as an acid–base type of exchange reaction:

$$A_xM_yO_z + xH^+ \rightarrow H_xM_yO_z + xA^+$$

$$(A = \text{alkali metal; } M = \text{transition metal})$$

This has been shown to occur for a great variety of mixed oxides such as titanates, niobates, tungstates, *etc.* and, although some reactions take place in pure water at room temperature, most of the reported cases need stronger conditions: hot nitric acid and sometimes pressure (hydrothermal) are also needed.[3–9]

As regarding layered AMO_2 materials (A = Li, Na; M = V, Cr, Co, Ni), the structures of which are α-$NaFeO_2$-type, acid exchange has been reported.[10–13] As is well known, the α-$NaFeO_2$ structure is one of the three possible superstructures of the rock-salt type where sodium and iron cations are ordered in alternating close-packed layers between oxide ion layers to form a rhombohedral structure (space group $R\bar{3}m$; see Fig. 1). Interestingly enough, the structure prototype, α-$NaFeO_2$ itself, does not behave in the same way because of its instability towards hydrolysis, hematite α-Fe_2O_3 being formed as the reaction product.[14]

An alternative approach is the use of molten organic acids as the proton source and reaction media. In this connection, Poeppelmeier *et al.*[15] have reported the reaction of $LiAlO_2$ with molten benzoic acid at 200 °C, which produces an almost lithium-free material of composition $Li_{0.05}H_{0.95}AlO_2$. The structure also changes from the α-$NaFeO_2$ type to the spinel type. Benzoic acid was chosen because of its relatively high boiling point (249 °C), moderately high acidity constant and low solubility of iron oxides in it.

Bearing all this in mind and searching for a possible new iron oxyhydroxide, we have performed similar reactions with benzoic acid and α-$NaFeO_2$. Although the synthesis strategy is the same, the results are significantly different: our X-ray diffraction, IR, Mössbauer and magnetization data suggest that the ferrimagnetic product of the exchange shows oxyhydroxide character with the spinel structure.

Moreover, in our case, some organic species (benzoates) are included, probably coordinated at the active surface sites and their elimination is quite difficult.

Finally, it is worth recalling that the dehydration by thermal treatment at moderate temperatures, in a second step, of the acid-exchanged products may result in new oxides.[16,17] In our

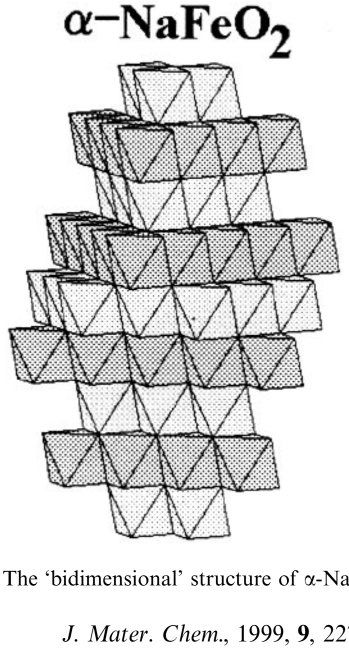

Fig. 1 The 'bidimensional' structure of α-$NaFeO_2$.

---

† Basis of the presentation given at Materials Chemistry Discussion No. 1, 24–26 September 1998, ICMCB, University of Bordeaux, France.

case, treatments at 300 °C of the intermediate oxyhydroxide yields the well known maghemite γ-Fe_2O_3, although some hydroxyl groups may still be present and its morphology, quite different from the usual acicular shape, is platelet-like.

Experimental

The exchange reactions were performed on molten benzoic acid at 150 °C for 24 hours either in an open flask, or in a sealed Pyrex ampoule, the best materials being obtained in the second case. A typical reaction used 1 g of α-$NaFeO_2$ and 50 g of benzoic acid, the mixture being stirred and most of the remaining acid being decanted upon finishing the experiment. The solid product, which from here on will be referred to as 'FeOOH', was thoroughly washed by a flow-back treatment with methanol in a first step and using hot water in a second step. In order to ensure complete removal of the organic matter, portions of the samples were treated for 24 hours with boiling 2 M NaOH solution.

Powder X-ray diffraction patterns were recorded with Cu-Kα radiation ($\lambda = 1.5418$ Å) filtered with Ni using a Philips X'Pert diffractometer operating at 40 kV and 40 mA. Data were refined by means of the FULLPROF program[18] based on the Rietveld method.[19]

Chemical analysis was performed by inductively coupled plasma (ICP) in a Jovin Yvon instrument (JY-70 plus) and thermoanalytical experiments (TG and DTA) were performed in a Stanton (STA-781 model) thermobalance with a heating rate of 10 °C min^{-1} from room temperature to 600 °C.

Magnetization measurements were performed at room temperature on a DSM-8 susceptometer of a maximum magnetic field of 12 kG. Mössbauer spectra were recorded in a conventional spectrometer working at constant acceleration mode with ^{57}Co in a rhodium matrix as radioactive source; the data analysis was made using the NORMOS program.[20]

IR spectra were recorded in a Nicolet 5SX apparatus fitted with caesium iodide optics, samples being diluted in KBr for transmission experiments. A diffuse reflectance infrared Fourier transform (DRIFT) cell (Spectra Tech model) fitted with a high temperature chamber (0030-103 model) was required for certain experiments. Data analysis was done by using the OMNIC 2.1 program from the Nicolet Instrument Corp.

Results and discussion

X-Ray diffraction

XRD patterns of the exchanged samples (Fig. 2) are very different from that corresponding to the pristine material. They show a profile characteristic of a cubic spinel-type material although some α-Fe_2O_3, hematite (7%) is also present. The amount of hematite is significantly lowered when the synthesis is performed in sealed ampoules but it could not be completely eliminated in our experiments, even under dry conditions. It seems then that the formation of this very stable oxide may occur by *in situ* dehydroxylation of the exchange product 'FeOOH'.

Although X-ray diffraction can not be used to identify hydrogen, Rietveld analysis was performed in order to confirm the spinel character of the structure as well as the iron distribution assuming a full oxygen stoichiometry. Table 1 collects the final structural parameters which show that iron is entering both the tetrahedral (8a) and octahedral (16d) positions but an important amount of cationic vacancies do also exist. Taking into account that oxide and hydroxide anions cannot be distinguished by X-ray diffraction, the best fit was obtained for the composition: $Fe_{0.86}$(tet.)$Fe_{1.14}$(oct.)$O_2(OH)_2$. In this connection, it is worth recalling the close structural relationships existing between the rock-salt and the spinel structures, which have been shown both theoretically and experimentally.[21,22] In fact, the sodium–proton exchange on α-$NaFeO_2$, assuming that protons would form OH^- anions, would empty half of the octahedral positions present, besides all the tetrahedral positions already vacant in the rock-salt structure and, with this scenario, iron cations would diffuse even at moderate temperatures to build up a spinel framework. In this connection, iron redistribution giving rise to spinel structures from alkaline ferrites by cationic exchange has been documented.[16,22] Note that the XRD pattern of the material after treatment with 2 M NaOH and heating at 300 °C in air looks very similar to that corresponding to the cubic form of γ-Fe_2O_3, maghemite.

Chemical analysis

Chemical analysis was performed in order to determine the amount of residual sodium, only minor amounts (1.3%) being found. On the other hand TG experiments were performed in order to detect weight losses from any iron oxyhydroxide present. Fig. 3 shows this to happen in air in two steps (*ca.* 20%), below 200 °C and 400 °C respectively, the second one being accompanied by a very strong exothermic effect in the

Table 1 Structure parameters of exchanged sample

Atom	Site	*x*/*a*	*y*/*b*	*z*/*c*	Occupation
Fe	8a	0.0	0.0	0.0	0.86(1)
Fe	16d	5/8	5/8	5/8	1.14(1)
O	32e	u	u	u	4.00(1)
Structure parameters	$u = 0.381(1)$; $a = 8.362(2)$ Å				
Rietveld refinement factors	$R_B = 9.13\%$; $R_p = 9.05\%$; $R_{wp} = 12.4\%$; $R_{exp} = 6.16\%$; $\chi^2 = 4.05$; Spinel phase: 93% (remainder: hematite phase)				

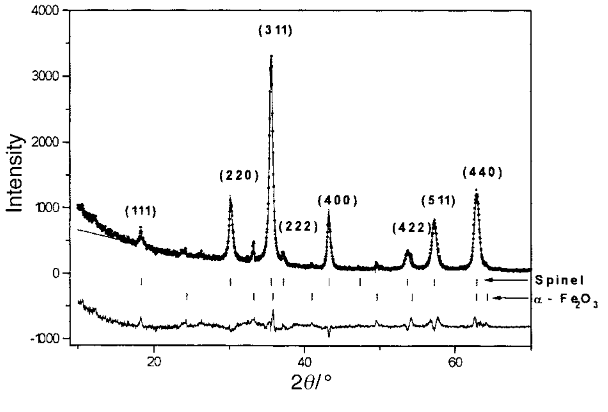

Fig. 2 X-Ray diffraction pattern of the exchange sample.

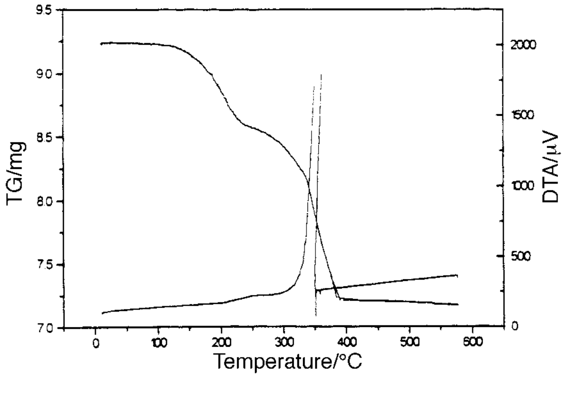

Fig. 3 Thermogram in air of the exchange sample.

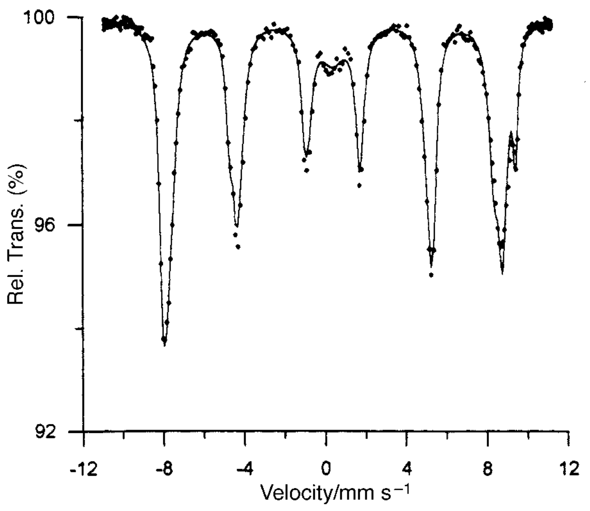

Fig. 4 Mössbauer spectra collected in N_2 (1) of the exchange reaction sample with benzoic acid.

Table 2 Hyperfine Mössbauer parameters in N_2 (1)

Position	δ/mm s^{-1}	ΔQ/mm s^{-1}	H/T	Population of Fe^{III}
Spinel phase				
Octahedral	0.43	−0.07	52.3	45%
Tetrahedral	0.41	0.00	49.6	41%
Hematite phase				
Octahedral	0.52	0.46	53.4	

DTA plot which disappears when the experiments are performed in flowing nitrogen. This is, as confirmed later by IR experiments, due to the combustion of some organic matter. Neither this exothermic effect nor such big weight losses are observed for samples washed with hot sodium hydroxide although this treatment may also eliminate most of the structural hydroxyl groups which, in fact, are of acidic character.

Mössbauer analysis

Mössbauer analysis was used to confirm the iron oxidation state and distribution as deduced from X-ray diffraction. Spectra were collected at room temperature and 77 K although quality fits were only obtained in the second case due to the low crystallinity which is inherent in the preparation method (Fig. 4). At zero velocity the appearance of residual, non-crystalline spinel persists even at 77 K. The relevant hyperfine Mössbauer parameters are reported in Table 2. The agreement with diffraction and magnetization data is quite satisfactory. A residual amount of hematite (*ca.* 14%) can be detected.

Magnetization

Magnetization *vs.* temperature curves were recorded at room temperature (Fig. 5) and are typical of ferrimagnetic ordering, an effective magnetic moment of 0.67 μ_B (at RT) per formula unit being obtained. This experimental value is in good agreement with the theoretical one, 0.70 μ_B, as deduced assuming the Néel collinear model: $[Fe_{0.86}]_{tet}\downarrow[Fe_{1.14}]_{oct}\uparrow$.

IR Spectroscopy

IR spectroscopic studies were performed aiming to ascertain the oxyhydroxide nature of the exchange product and to follow the dehydration process.

Fig. 6 presents the spectra of the original α-$NaFeO_2$ and its reaction product with benzoic acid. As regarding the pristine material, besides the characteristic Fe–O lattice vibrations, a strong band appears at 1483 cm^{-1} which can be attributed to carbonate and/or hydrogencarbonate groups. Nevertheless, sodium ferrite is almost pure and, in this connection, it has to be recalled that one of the components used for its synthesis, sodium peroxide, is very sensitive to CO_2 and, therefore, minor amounts of superficial carbonates which do not affect the overall reaction are present. As is well known, their corresponding IR vibrations are very intense because they exhibit strong variations in the dipolar moment. On the other hand, some hydroxyl groups are also present (*ca.* 3400 cm^{-1}).

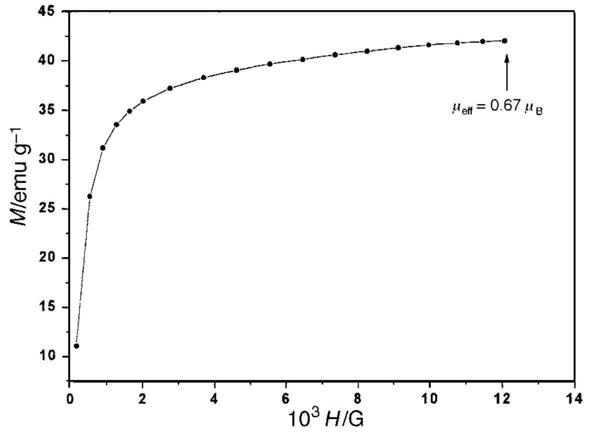

Fig. 5 Magnetization at saturation of the reaction product with benzoic acid.

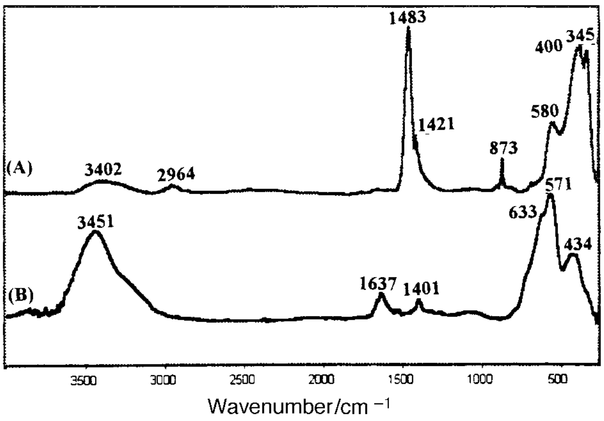

Fig. 6 Transmission spectra of α-$NaFeO_2$ (A) and its reaction product with benzoic acid (B).

Multicomponent bands in the Fe–O vibration region (800–300 cm^{-1}) are shown in both spectra but there are clear differences at the maximum frequencies and relative intensities for each one, which indicate that a structural transformation took place. A certain degree of similitude of the band arrangement for different iron oxide phases is expected due to their common structural features (*e.g.*, all of them present FeO_6 octahedral units). This fact frequently makes it difficult to unambiguously assign each band of the infrared spectral region with a normal vibration mode of a specific phase. Nevertheless, taking in account the presence of FeO_4 tetrahedral structural units in the spinel ferrites, we must expect to observe in the IR spectrum additional characteristic vibrations at higher frequencies[23] than those of the iron oxide phase formed exclusively by FeO_6 polyhedral units (α-$NaFeO_2$). In accordance with this point, the spectrum of the reacted sample shows a shift of the complex Fe–O vibration band toward higher wavenumbers. In this context, it is very indicative of the formation at 633 cm^{-1} of the shoulder, which is characteristic of the iron oxide phase with spinel structure, as is shown in Table 3.

Table 3 Main infrared bands of different iron oxide compounds

Compound	Wavenumber/cm^{-1}						
α-NaFeO$_2$		580 (ms, b)		400 (s)		345 (s)	
α-Fe$_2$O$_3$ (ref. 24)		560 (s, b)	468 (s)		370 (sh)		325 (s)
Fe$_3$O$_4$ (ref. 25)	633 (s, d)	590 (s, d)	445 (m, d)	404 (m, d)	358 (sh)		
Exchange sample	633 (s, sh)	571 (s)		434 (m)		352 (w, sh)	

(s) strong, (m) medium, (w) weak intensity, (b) broad band, (sh) shoulder, (d) doublet.

Therefore, the comparative study of the infrared spectra of both samples indicates that the reaction of α-NaFeO$_2$ with benzoic acid results in spectral modifications consistent with the transformation of a structure with an FeO$_6$ polyhedral arrangement into another having FeO$_6$ and FeO$_4$ polyhedral units.

Study by diffuse reflectance of the hydroxyl spectral region of the reacted sample. Fig. 7 shows the hydroxyl region of the DRIFT spectra of the reacted sample. The room temperature spectrum presents a broad and strong band centered at about 3440 cm^{-1} related to the stretching vibrations of the hydroxyl groups of the sample. The broadness of this band and the frequency of its maximum do not allow in principle any specific assignment. Therefore, the presence of hydration and/or crystallization water and structural hydroxyl groups may be considered. Nevertheless, it is important to note the concordance, in shape and frequency, of this band with those of some iron oxyhydroxide phases.[26,27]

In order to gain insight into the structural origin of this band, the sample was heated in a temperature controlled DRIFT cell to 450 °C, and diffuse reflectance spectra were taken every 50 °C. It is observed that the band of the sample heated at 150 °C still has a strong intensity, indicating that the band is not produced by hydration water, which would be removed at this temperature.

On the other hand, when the temperature was increased from 200 to 400 °C a continuous decrease of the band intensity was observed, although significant intensity remains even at 400 °C. Such behaviour is interpreted as a strong indication that this band is related to structural OH groups. In effect, the continuous loss of intensity over a wide temperature range is in good agreement with a dehydroxylation process which occurs in precisely this way, while the loss of crystallization water takes place at a narrower temperature interval. A similar argument may be used to eliminate the possibility of this band being associated with the OH of the methanol contamination of the sample, which is removed at 250 °C, or with the remaining benzoic acid which is observed at 2900 cm^{-1} far from the 3440 cm^{-1} band under study. In addition, the spectrum of the sample treated above 300 °C shows two medium intensity bands centered at 3600 and 3800 cm^{-1} which are typically assigned to surface OH groups.[28]

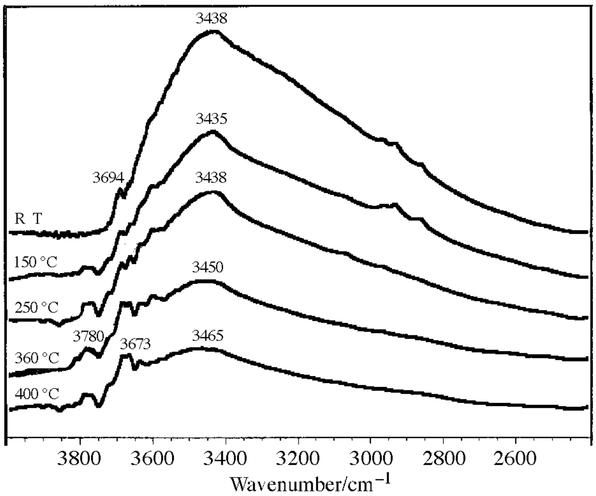

Fig. 7 OH region DRIFT spectra of the reacted sample.

The results of the absorption and DRIFT spectra suggest that the reacted sample is an iron oxyhydroxide phase with the spinel structure, having structural and surface OH groups.

Comparison of the Fe–O vibrations of the reacted sample after thermal treatments at 300 and 600 °C. Fig. 8 presents the Fe–O bands of the reacted sample and the corresponding products after thermal treatments at 300 and 600 °C. The spectra of the original sample and that treated at 300 °C present the same band arrangement, the only difference being that the shoulder about 630 cm^{-1} has a better definition for the sample treated at 300 °C. Knowing that this shoulder is characteristic of the iron oxide phases with the spinel structure, the treatment at 300 °C seems to improve the crystallinity of the spinel phase which can now be identified as maghemite, γ-Fe$_2$O$_3$, although a small amount of OH$^-$ groups seem to be present. The spectra of the corresponding samples where organic matter has been completely eliminated by alkaline treatment are very similar to these.

In contrast, the spectrum of the sample treated at 600 °C shows a general shift of the whole complex Fe–O band towards lower wavenumbers, while at the same time the shoulder at about 630 cm^{-1} becomes smaller and three new bands appear at 463, 389 and 331 cm^{-1} in agreement with the expected frequencies for the α-Fe$_2$O$_3$ phase (Table 3), a result that is also confirmed by XRD analysis. These facts indicate that the treatment at 600 °C of the original sample results in the formation of α-Fe$_2$O$_3$ at the expense of the partial loss of the spinel phase.

The authors are gratefully indebted to Dr. U. Amador (Universidad CEU-San Pablo, Madrid) for helpful discussions; to Dr. R. Rojas (I.C.M. Madrid), for performing thermal analysis and to Dr. M. T. Larrea (U.C.M.) for ICP

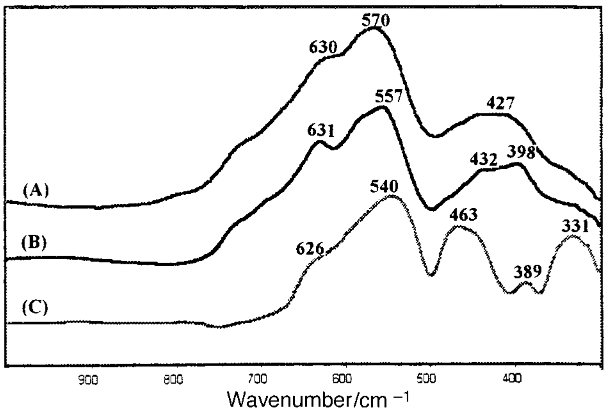

Fig. 8 Fe–O vibrations of the original reacted sample (A), reacted sampled treated at 300 °C (B), and reacted sample treated at 600 °C (C).

analysis. Financial support was provided by the Spanish Ministery for Education (CICYT, Project MAT 95-0809).

References

1 W. A. England, J. B. Goodenough and P. J. Wiseman, *J. Solid State Chem.*, 1983, **49**, 289.

2 S. Chandra, *Superionics Solids: Principles and Applications*, North-Holland, Amsterdam, 1981, p. 46.

3 R. Marchand, L. Brohan, R. Mbedi and M. Tournoux, *Rev. Chim. Miner.*, 1984, **21**, 476.

4 R. Marchand, L. Brohan and M. Tournoux, *Mater. Res. Bull.*, 1980, **15**, 1129.

5 B. Raveau, *Rev. Solid State Sci.*, 1988, **1**, 515.

6 A. J. Jacobson, J. T. Lewandowski and J. W. Johnson, *J. Less-Common Metals*, 1986, **116**, 137.

7 J. Gopalakrishnan and V. Bhat, *Inorg. Chem.*, 1987, **26**, 4300.

8 S. Byeon, J. Yoon and S. Lee, *J. Solid State Chem.*, 1996, **127**, 119.

9 S. Uma, A. R. Raju and J. Gopalakrishnan, *J. Mater. Chem.*, 1993, **3**, 709.

10 J. M. Fernández, L. Hernán, J. Morales and J. L. Tirado, *Mater. Res. Bull.*, 1988, **23**, 899.

11 L. Hernán, M. Macías, J. Morales, J. Pérez-Vicente and J. L. Tirado, *Mater. Res. Bull.*, 1989, **24**, 781.

12 J. Morales, J. Pérez-Vicente and J. L. Tirado, *Mater. Res. Bull.*, 1990, **25**, 623.

13 M. G. S. R. Thomas, W. I. F. David and J. B. Goodenough, *Mater. Res. Bull.*, 1985, **20**, 1137.

14 M. C. Blesa, E. Morán, N. Menéndez, J. D. Tornero and C. Torrón, *Mater. Res. Bull.*, 1993, **28**, 837.

15 R. Poeppelmeier and D. O. Kipp, *Inorg. Chem.*, 1988, **27**, 766.

16 C. Barriga, J. Morales and J. L. Tirado, *Mater. Res. Bull.*, 1990, **25**, 997.

17 J. Rouxel, *J. Solid State Chem.*, 1973, **17**, 223.

18 J. Rodríguez-Carvajal, FULLPROF: A Program for Rietveld Refinement and Pattern Matching Analysis, Abstract of the Satellite Meeting of the XVth Congress of the International Union of Crystallography, Toulouse, France, 1990, p. 127.

19 H. M. Rietveld, *J. Appl. Crystallogr.*, 1969, **2**, 65.

20 R. A. Brand, *Nucl. Instrum. Methods Phys. Rev. B*, 1987, **28**, 398.

21 Y. A. Kesler and D. S. Filimonov, *Inorg. Mater.*, 1994, **30**, 1255.

22 M. C. Blesa, E. Morán, U. Amador and N. H. Andersen, *J. Solid State Chem.*, 1997, **129**, 123.

23 J. Preudhome, *Sémm. Chim. État Sol.*, 1974, 31.

24 N. T. McDevit and W. L. Baun, *Spectrochim. Acta*, 1964, **20**, 799.

25 M. E. Mata-Zamora, MSc Thesis, Facultad de Ciencias, UNAM, México D.F., 1998.

26 T. Ishikawa, S. Nitta and S. Kondo, *J. Chem. Soc., Faraday Trans. 1*, 1986, **82**, 2401.

27 C. H. Rochester and S. A. Topham, *J. Chem. Soc., Faraday Trans. 1*, 1979, **75**, 872.

28 H. Watanabe and J. Seto, *Bull. Chem. Soc. Jpn.*, 1993, **66**, 395.

Paper 8/05540H